International Conference on Advances in Structural and Geotechnical Engineering

ICASGE'17

27-30 March 2017, Hurghada, Egypt

EXPRIMENTAL INVESTIGATION ON THE BEHAVIOR OF SIGMENTALBOX GIRDER BRIDGES WITH EXTERNAL PRESTRESSING UNDER COMBINED SHEAR, MOMENT AND TORSION

Tarek El-Shafiey[1], Abdel-Hakeem Khalil[2], Emad Etman[3], Mahmoud Abelaziz[4]

[1,2,3] *Professors, Faculty of Engineering, Tanta University, Egypt*

[4] *Assistant lecturer, Faculty of Engineering, Tanta University, Egypt*

E-mail: Eng.mahmoud_abdelaziz@yahoo.com

ABSTRACT

Currently, segmental box girder bridges with external prestressing is widely used in construction all over the world. This paper presents experimental test results on five specimens represents a box girder bridges with external prestressing taken with one-tenth scale. The specimens were simulated to the internal negative moment zone bounded by contra flexure point as cantilever specimen. All specimens are segmental beams with dry-keyed joints and they were tested under; bending, shear and torsion. Applied load eccentricity which causing torsion variation and tendon prestressing force level are the two main studied parameters. The behavior of the beams was evaluated in terms of; load open critical joint, cracking load, ultimate load, deformations such as deflections, twist angle and joints opening width as well as, strains of external tendons and internal steel. Also, behavior of the specimen including modes of failure, cracks propagation history and some critical values are also discussed. Some important remarks also are presented. The experimental results showed that, the existing of torsion has significant effect on the beams cracking behavior, deformed shape, mode of failure, and has slight effect on increasing the prestressing tendon stress at eccentric applied load side more than the side far from the applied load. Also, increasing effective prestressing force level has a significant effect to delay cracking due to shear stresses, and improve the beam deformation against flexure and torsion. Also, it has slight effect to reduce the difference between tendon stress at every side.

Keywords: behavior, Segmental, box, girder, External, prestressing

INTRODUCTION

Segmental bridges with external prestressing have been widely built due to its construction facilities. Using minimum internal reinforcement in segments which improve the concreting operation, profile of main external steel is easier to check, external tendon or deteriorated segments can be removed and replaced, friction loses can be reduced, concreting and prestressing are now independent operations, minimum construction time can be achieved and no cracks is a result of using this construction method, Rombach [1].

Because of the tendons are outside of the structure and linked only at anchors and deviators, the analysis of a concrete member with external tendon is complicated. Because, there is no compatibility between concrete and prestressing steel strains. Also, under loading and after the joint opening, the connected parts between segments in compression zone can transfer the applied load by compression and friction. External tendons only can resist the tension force at tension zone. Internal steel didn't contribute in tension at joints because it doesn't cross the joint. At ultimate stage, the neutral axis depth is decreased due to moment increase, the compression zone area is much smaller and external tendons contribution to resist tension force decreases due to shortage of tendon eccentricity (second order effect). The load carrying capacity of the joint decreases gradually and applied load increased until reached each other at failure.

From the codes [2]–[6] provisions and history of segmental construction, international codes suggested design limitations for segmental bridges with external prestressing because of wide spread of these constructions to be controlled by the specifications. When dry joint is used, codes suggested to design these structures at service stage to have closed joints (full prestressing stage). In segmentally constructed bridges due to the sum of effective prestressed and permanent loads the compression stress must not exceeds 0.45 f'c. Also, recommended that at any place on the cross-section where the axial tension due to torsion and bending exceeds

the axial compression due to prestressing and bending, either supplementary tendons to counter the tension or local longitudinal reinforcement, which is continuous across the joints between segments, shall be required. Several researches were constructed to study the behavior of segmental beams under moment [1], [7]–[28] and shear[29]–[32]. The aim of these researches is to get benefit from the nonlinear stage and design these types of structures at the ultimate stage which reflected on the total cost of the structure and less use of materials. Bridges is different from beams because of the load can moving along the beam and in the cross-section direction. The unbalanced loading of the bridge deck in its cross-section direction can generate torsion. At the negative moment zone, the dry joint will have suffered from combined straining actions; moment, shear and torsion. This paper was constructed to fill the shortfall of behavior of segmental bridges with external prestressing subjected to moment, shear and torsion. The specimens were simulated to the internal negative moment zone bounded by contra flexure point as cantilever specimen. Section at contra flexure point as free end on the other hand section at maximum negative moment as fixed end.

REVIEW OF PREVIOUS RESEARCH

Several studies had been conducted to study the behavior of externally prestressed concrete beams with external prestressing. The largest number of researches focused on flexural behavior[1], [7]–[28]. The analysis of segmental beams at various stages and ultimate flexural resistance is still need more researches. Limited number of papers studied the behavior of the simply supported beams under combined straining actions by Algorafi et al [33]–[36]. He studied experimentally the behavior of externally prestressed segmental beam under torsion [34]–[36] based on one experimental program. Another paper [33] studied externally prestressed monolithic and segmental concrete beams under torsion using finite element program. It is worth mentioning that, Algorafi et al [33]–[36] studied the beam with strait and harped tendon, flat and keyed joint. The specimen consists of three segment along the beam length which cannot be simulated to the implementation. The keyed joint has only one shear key at every web. But in fact, when the torsion occurs, the designer will use max number of shear keys to transmit the maximum amount of shear flow across the joint. The modes of failure and laboratory data also for all beam influenced by cracks at anchorage and deviators.

EXPERIMENTAL PROGRAM

The main objective of the present part is describing the overall scheme of the paper which is mainly conducted to study the behavior of one-tenth scale specimens of segmental box girder bridges (S.B.G. B) with external pre-stressing (E. P) under combined straining actions (Moment, shear and torsion). The experimental program consisted of five specimens divided into two groups I and II. The main aim of group I is to study the effect of different load eccentricity causing torsion level (e_1=0.05m, e_2=0.2m and e_3=0.4m) at constant high level of pre-stressing forces (tendon strain ε_{ps3}=4100 micro strain (μs) which means that the effective prestressing force P_e=0.5P_{yps}). The main aim of group II is to study the effect of different tendon pre-stressing force (with effective strains ε_{ps1}=2100 μs or P_e=0.5P_{yps}, ε_{ps2}=3100 μs or P_e=0.38P_{yps} and ε_{ps3}=4100 μs or P_e=0.26P_{yps}) at constant high eccentricity of applied load (e_3=0.4m). The prestressing level is main parameter which prove that it can affected the mode of failure, Huang [30]. Table 1 shows the studied parameters.

Table 1 The main studied parameters.

Group	Specimens	Applied torsion level (kN.m)	Prestressing level from yield strength
GI	S1s-0.5Pys-0.05P	0.05 P	P_e=0.5P_{yps}
	S2s-0.5Pys-0.2P	0.20 P	P_e=0.5P_{yps}
	S3s-0.5Pys-0.4P	0.40 P	P^e=0.5P_{yps}
GII	S3s-0.5Pys-0.4P	0.40 P	P_e=0.5P_{yps}
	S4s-0.38Pys-0.4P	0.40 P	P_e=0.38P_{yps}
	S5s-0.26Pys-0.4P	0.40 P	P_e=0.26P_{yps}

Specimen dimensions.

The tested specimens were one-tenth scale and represented a negative moment zone bounded by section at maximum negative moment and section at contra flexure point. To have good fixation of the specimen in

laboratory at testing, the box girder beam is used from one side with extended fixation block from top and bottom of the beam. Each specimen has five segments; Fixation block with solid connected part, three segments of tenth scale B.G.B and the end block segment with solid connected part. The Fixation block dimension is 2.10 m length and cross section of 0.3m x 0.75m. It has a monolithically casted solid part of 50 mm length with the same dimension of the beam to avoid failure at Fixation block face and to have free distance to fix the pi-shape used to read the strains in concrete. The three segments of B.G.B are hollow box section with upper flange 750 mm wide and lower flange with 450 mm wide. The depth of the girders is 360 mm. The upper slab, the horizontal slab and the girder is with 80 mm thickness. Each B.G.B segment is with length equal to 0.30 m. The end solid block dimension is 1.10m length and 0.36m x 0.30 cross section. It is casted monolithically with solid part of 50 mm length with the same dimension of beam like the Fixation block. The Fixation block, end block and beam section lay out is shown in fig. 1. Fig 2, shows the beam cross section details. The shear keys are distributed by three shear keys at every web, five at larger flange and three at smaller flange. The shear keys are with base dimension of 40 mm x 80 mm and with angle of 55 ° and projected with 12.5 mm, Fig 3 shows the beam cross section and shear keys distribution. All specimen dimensions shown in fig. 4.

Specimens' reinforcement detailing

The internal reinforcement for the Fixation block is 12 bar with 16mm diameter and 14 stirrups with 8mm diameter to avoid the deformation of Fixation block or cracking. The connected solid part to Fixation block reinforced with one stirrup and the same longitudinal reinforcement as the beam segments as shear connector. Every segment is reinforced with minimum steel for longitudinal and transversal steel. The longitudinal steel is 14 bar with 12 mm diameter. The transversal steel is two stirrups with 8 mm diameter. The end block part is reinforced with 4 bars with 16 mm diameter in tension side to avoid flexure cracks to this part and 4 bars with 12 mm diameter in compression side. The stirrups were 7 stirrups with 8 mm diameter which designed also to avoided any cracks in shear. Fig. 5 illustrate the details of the reinforcement of beam segment.

Material properties

A concrete mix was designed to give an average cube crushing strength after 28 days (f_{cu}) equals to 40 MPa. It consists of 500 kg cement, 387.5kg sand, 1175 dolomite, 0.28 water cement ratio and 8.0 Littre super plasticizer for 1.0 m^3 of concrete. Tension tests by the universal testing machine were performed on standard specimens to obtain the stress-strain curve for both used deformed, smooth bars and tendons. The actual yield stress for the used deformed bars of 12 mm was 420MPa. Smooth wires having a diameter of 8mm, were of actual yield stress 285MPa. The used tendon with 15.24 mm^2 diameter and standard area of 154 mm^2. The actual yield stress for the used tendons was 1696 MPa.

Fabrication of specimens

The Fixation block was casted first on flat concrete floor covered by bully-wood shuttering after reinforcement cage had been laid. To have no separated layers between Fixation block and the 50-mm connected solid part, it has been casted with leaved rough surface of Fixation block at the second day after painting the surface with adhesive material. shear keys gapes are formed by fabricated wood stamps with the dimension shown before. After one day, the stuttering of the beam segments no.1 is formed. Foil papers used to separate concrete of each segment. Foams is used to form the hollow section. A steel gage is laid to the shuttering. Electrical strain gages were mounted on the reinforcement at several positions at longitudinal and transversal steel. the first segment is concreted and botom shear keys was formed automatically by matching bottom serface. Finally, and after casting, the top shear keys gapes is formed by using fabricated wood stamps. Concreting segment 2 and 3 has been passed with the same steps .Fig. 6 shows this step. The solid part connected to end block and the end block were casted finally together

Fig. 1 specimen lay out

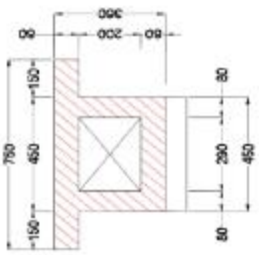

Fig. 2 beam cross section and dimension

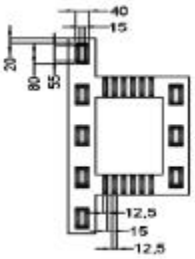

Fig 3 shear keys distribution and dimension

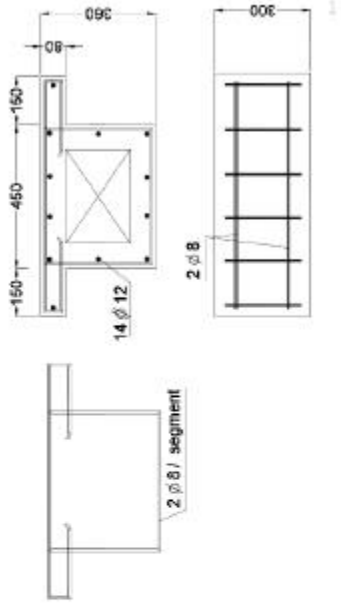

Fig. 4 specimen dimensions

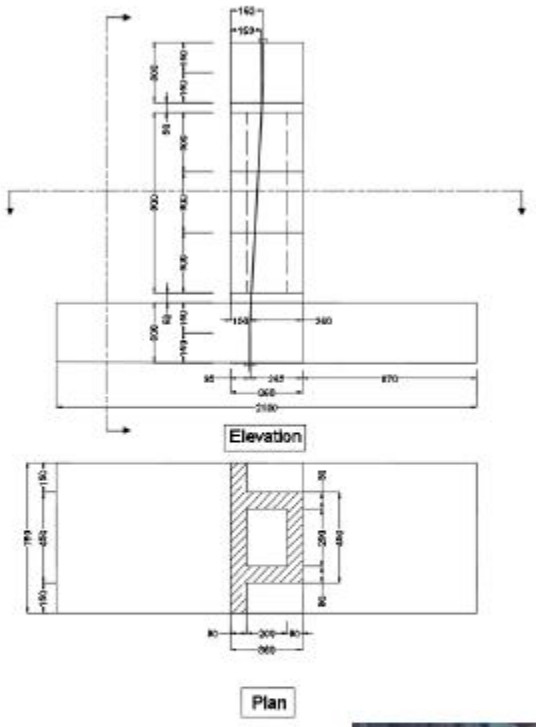

Fig. 5 beam segment reinforcement

Fig. 6 formation of shear keys at joints

Testing setup and instrumentations

Every segment is removed from the form after one day and were moist-cured for 10 days. The average age of specimens at time of testing was about 28 days. All specimens are transferred from the casting place to testing place by clerk. It's worth mentioning that, the specimen S1 exposed to destabilize during transfer operation which resulted in existence of some impurities and absence of exact match between surfaces at the first joint. The test program was performed in the Reinforced Concrete Laboratory of the Faculty of Engineering, Tanta University. After specimens curing, every specimen passed through two faces, post-tensioning face and testing

face. Table 2 shows the prestressing results of the tested specimens and its notation. The recorded prestressed strains is read from electrical resistance strain gauges mounted on surface of the external tendons at mid-length. One of the major aspects of this paper is to get more complete information on behaviour of segmental box girder bridges with external prestressing under combined stresses. So, the instrrumentations was located at relevant points of the test specimens. The deformation may be measured by LVDTs and concrete strains may be measured by pi-gages. LVDTs is used to mesure the deformation at four points as shown in Fig. 7 .Four pi-gagues, 100mm length, were mounted on the surface of the specimen at different locations as viewed in Figs. 8. Also, electrical resistance strain gauges were mounted on the surface of the longitudinal reinforcing and transversal stirups as shown in Figs. 9 for steel of first segment. A Steel supporting elements was specially designed and fabricated for performing the test program. First, four channels no. 200 is fixed to the frame bottom beam with 16 bolts, 18 mm diameter. Steel plats is installed over the channels edge. The specimen, a hydraulic jack for applied load at the end block and a hydraulic jack for stability load at Fixation block is installed. For alignment of the tested specimen and to insure uniform bearing stresses at the supports, a quick set gypsum was used at the support plates. Gypsum was also used to align and secure the loading plates at the used hydraulic jacks. The stability load at Fixation block was applied incrementally in an increment of 25 kN up to reaches 250 kN measured by the load cell attached to the mechanical jack. Four channels no. 200 is put over the Fixation block and fixed to bottom channels with 16 bolts, 18 mm diameter. The LVDTs were adjusted, and the strain gauges as well as pi-gauges, were connected to data acquisition system, then checked for correct readings. The readings of all LVDTs, strains, and pi-gauges were then recorded for zero load. The applied load was applied incrementally in an increment of from 1.0 to 5.0 kN up to failure and measured by the load cell attached to the manual jack. The overall test setup shown in fig. 10

Table 2 The recorded exact strains for experimentally tested specimens.

Specimen notation	Prestressing level from yield strength	Required micro prestressing strain	Recorded micro Prestressing Strain for tendon near / far from the applied load	
S1s-0.5Pys-0.05P	$P_e=0.5P_{yps}$	4100	4113	4092
S2s-0.5Pys-0.2P	$P_e=0.5P_{yps}$	4100	4075	4036
S3s-0.5Pys-0.4P	$P^e=0.5P_{yps}$	4100	4108	4124
S4s-0.38Pys-0.4P	$P_e=0.38P_{yps}$	3100	3167	3147
S5s-0.26Pys-0.4P	$P_e=0.26P_{yps}$	2100	2116	2123

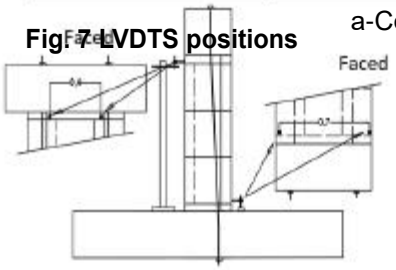

Fig. 7 LVDTS positions

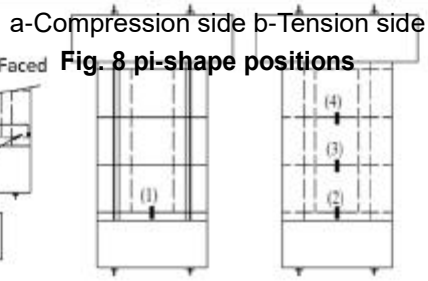

a-Compression side b-Tension side

Fig. 8 pi-shape positions

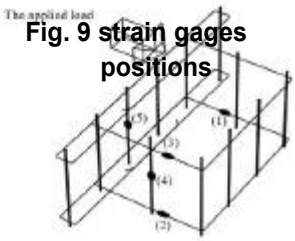

Fig. 9 strain gages positions

a. Test set up

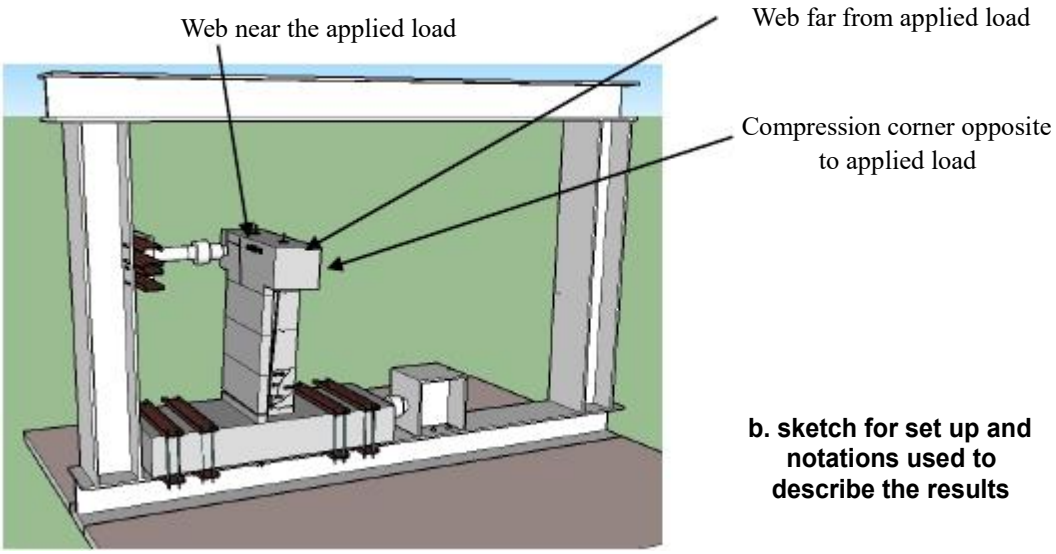

Fig. 10 Test setup

EXPERIMENTAL RESULTS, OPSERVATIONS AND RESULTS

The testing load was applied gradually until failure. The test results for all groups were analyzed and arranged in tables and graphical forms. Behavior of each specimen will have discussed in the following lines.

Cracking behaviour and modes of failure

This section will discuss the load cracking behavior for group I and group II. All cracks were marked on all sides of tested specimens up to failure. The value of the applied load was inscribed at the end of each crack. In this way, a complete crack propagation history was available from photographs taken after the test. The duration of each test was from 45 minutes to one hour. In general, there is no crack developed at the anchorages or deviators (end block or Fixation block)

GI: Figs. 11, 12 and 13 shows the sequence of specimen's failures of group I. In general, with increasing the applied loads the critical joint (dry joint at maximum moment) opened at load of 42, 42.5 and 42 kN for S1, S2 and S3 respectively from the laboratory tests.

For specimen with low torsion level, 0.05P, S1, after opening of first joint, with increase the applied load and near the ultimate load, small compression zone bounded by cracks developed at the first joint at the web near the applied load at approximately 80 kN as shown in Fig. 11b. At the same time, Compression failure take place sequentially along the compression zone at first joint starting from web near the applied load and ended with the web far from the applied load. The compression zone at web far from the applied load is larger than the web near the applied load. This is due to warping effect which decreases the neutral axis depth at web near the applied load. Fig. 11a. Fig. 11c shows the failure mechanism of the beam.

However, for the specimens S2 and S3 and after joint opening, hair crack occurs at the web far from applied load with angle 80^{o} and 65^{o} at load of 55 kN and 49.9 kN for S2 and S3 respectively. The cracks are developed because of, twisting of the first segment at tension face due to torsion and the restriction of twisting at the contact area in compression at the joint. The crack is stopped when the shear keys diagonal face at the joint is reached each other. Under loading the opening between joint at tension side increased, twisting deformation increased, the diagonal cracks at the web far from the applied load increased and stopped when shear keys contacted with each other. Figs. 12a and 13a shows the crack propagation at this face. a gradual degradation in stiffness was observed at this stage. This occurred as cracks developed due to twisting as well as joint opening due to moment. For specimen S2 and near the failure load of 78 kN, compression failure occurs at web near the applied load at the first joint followed by slight sliding at this web due to twisting resisted by small closing of joint opening and shear keys contact. Then, diagonal compression failure developed form the end of diagonal crack that developed at the web far from at compression flange to classify the mode of failure as compression failure. For specimen S3 and at the ultimate load of 64.6 kN, failure due to twisting take place and occurs as sliding of the web near the applied load followed by diagonal compression failure at the compression flange. Figs. 12b and 13b shows the crack propagation at the web near the applied load. Figs. 12c and 13c shows the cracks at web far from the applied load. The twisting make the tension flange reached the external tendons then, physical failure criteria is considered.

Fig. 11 Crack pattern of specimen (S1s-0.5Pys-0.05P)

Fig. 12 Crack pattern of specimen (S2s-0.5Pys-0.2P)

GII: Figs. 13, 14 and 15 shows the sequence of specimen's failures of group II. It is worth mentioning that, the specimen S3 common in GI and GII. In general, with increase the applied loads, the first joint open at load of 42, 32.6 and 26.18 kN (for S3, S4 and S5 respectively) from the laboratory tests. It is worth mentioning that, all specimens are with large torsion value. After joint opening, hair crack occurs at the web far from applied load with angle 65°, 68° and 70° at load of 49.9, 47.5 and 44.2 for S3, S4 and S5 respectively. The cracks developed with the same technique that showed before for S3 in GI. For all specimens in this group, and at the ultimate load of 64.6 kN, 57 kN and 49.3 kN for S3, S4 and S5 respectively, crushing of contacted shear keys and failure due to twisting take place and occurs as sliding of the web near the applied load. Figs. 13a, 14a and 15a shows the crack propagation at web far from the applied load. Figs. 13b, 14b and 15b shows the cracks propagation at web near the applied load. Figs. 13c, 14c and 15c shows the cracks developed at compression flange after high deformation. The twisting make the tension flange reached the external tendons then, physical failure criteria is considered.

Fig. 13 Crack pattern of specimen (S3s-0.5Pys-0.4P)

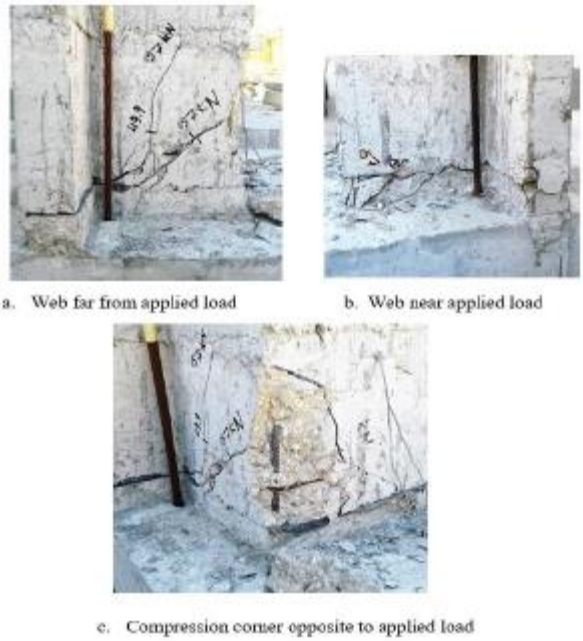

Fig. 14 Crack pattern of specimen (S4s-0.38Pys-0.4P)

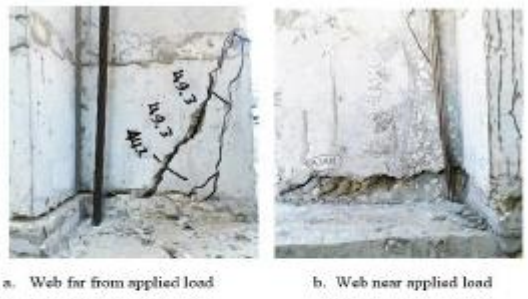

a. Web far from applied load b. Web near applied load

c. Compression corner opposite to applied load

Fig. 15 Crack pattern of specimen (S5s-0.26Pys-0.4P)

Deformation characteristics

This section will discuss the load deflection and load twist behavior for group I and group II. The deflection measured at central point at the end of beam segments. And the twist is calculated from two LVDT placed at the end of beam segment with 400 mm spacing. For all specimens, Initially the relationships were linear. Then, with increase of applied load, the response became nonlinear until failure. From the values of load at end of linear stage it's founded to be the same value of loads causing joint to open. That prove that, opening between segments at joints was the reason of the nonlinear behavior of segmental beams.

GI: Figs. 16, shows the load deflection curves. The relationship was linear up to vertical loads of 48.5, 48.5 and 49 kN (for S1, S2 and S3 respectively). These values prove that, opening between segments at joints wasn't the reason of nonlinear behavior of segmental beams. At this load level the external tenons strain starting to increase more than previous which means that tension stresses occurred at the dry joint at tendon levels. at this moment, the segment is rotated at the critical dry joints level at compression edges. To have sufficient compressed areas at the compression side, the concrete starts to achieve nonlinear behavior. The beam flexural stiffness is reduced due to shortage of compressed areas and concrete nonlinearity. After that, the response was nonlinear up to 80, 78 and 64.6 kN. Finally, failure occurs. From the values, it can be concluded that with increasing load eccentricity to increase applied torsion the linear part will not affected, because the flexure is the responsible to joint opening, but the ultimate load will decrease with slight decrease also in flexure stiffness in the nonlinear range. Figs. 17, shows the relationship between load and twist angle for all beam in GI. From the curves, it was observed that after the linear part, the twist angle of the beams would increase with increase in torsion. Consequently, the torsional stiffness for the beams with large eccentricity is decreased faster than beams with small eccentricity with load increase. Finally, with increasing the applied force eccentricity to increase the torsion effect, the ultimate load and ultimate deflection decreased, on contrary, the maximum twist increased.

GII: Figs. 18, shows the load deflection curves. The relationship was linear up to vertical loads of 49, 38.76 and 27.54 kN (for S3, S4 and S5 respectively). As GI, these values prove that, opening between segments at joints wasn't the reason of the nonlinear behavior of segmental beams After that, the response was nonlinear up to 64.6, 57 and 49.3 kN. Finally, failure occurs. In case of beam with large pre-stressing force S3 the relationship was linear up to 49 which was larger than other beams. the ultimate load of S3 was 64.6 which is the largest value. This is due to the normal force applied to the beam due to pre-stressing force of tendons. From the values, it can be concluded that with increasing pre-stressing force the linear stage and ultimate load will increase. Also, with increasing the prestressing force the ultimate deflection will slightly affected. The prestressing force has no effect on the flexure stiffness of the beams at the nonlinear stage. Figs. 19, shows the relationship between load and twist angle for all beam in GII. From the curves, at nonlinear part it was observed that, the twist angle of the beams would increase with increase in load. Consequently, the pre-stressing force has no effects on torsional stiffness at the nonlinear stage.

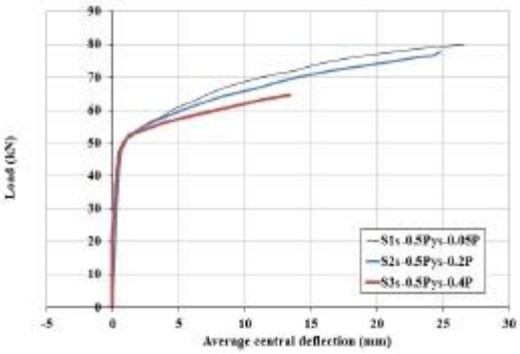

Fig. 16 Load vs. deflection for specimens in GI

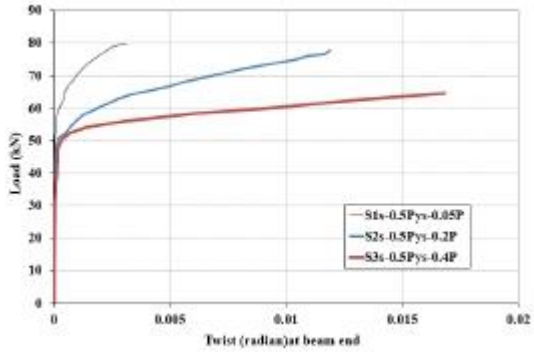

Fig. 17 Load vs. twist angle for specimens in GI

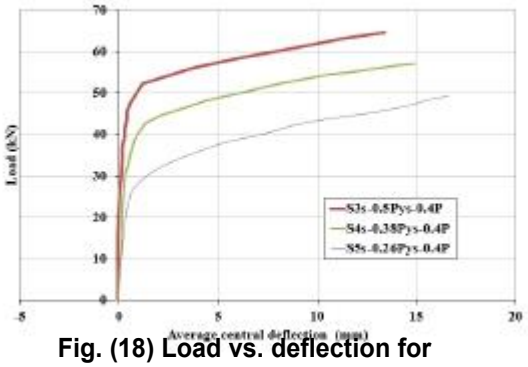

Fig. (18) Load vs. deflection for specimens in GII

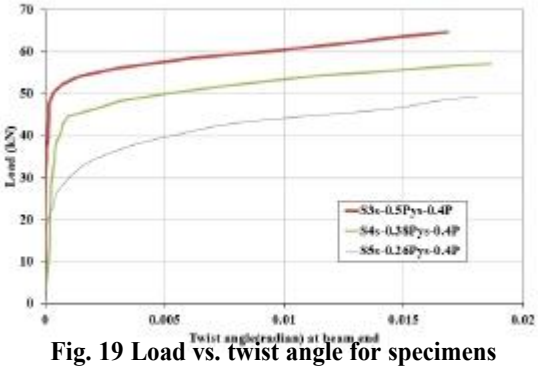

Fig. 19 Load vs. twist angle for specimens in GII

The main responsible for large amount of torsion is the opening of dry joint Fig 20 and 21 shows the measered twist for the beam after the dry joint directly. The figures is ploted with the same previous scale of load twist curves.

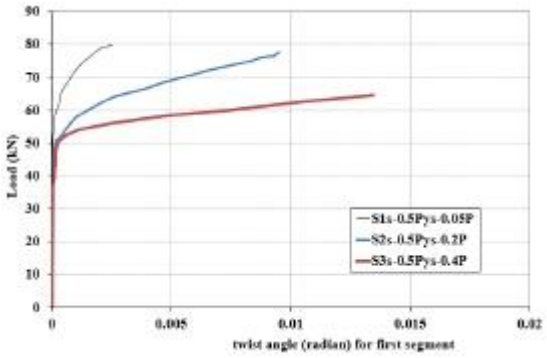

Fig. (20) Load vs. twist angle for specimens in GI after the dry joints

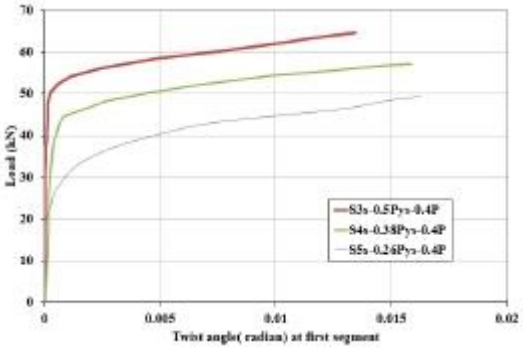

Fig. 21 Load vs. twist angle for specimens in GII after the dry joints

tendon strains

This section will take care of the variation of each tendons' strain (tendon near the applied load and tendon far from the applied load) with load for all specimens. Initially, the relationship was linear, and with a further increase in the applied load, the response became nonlinear. For all specimens, the strain of the tendon near the applied load increases more than the strain of tendon far from the applied load with increasing applied load as

shown in Figs. 22. a and b. Also, with increasing the applied load eccentricity to increasing torsion effect the difference between the tendons strain increased, this is because of warping due to torsion.

GI: Figs. 22. a shows Load plotted versus strain for tendon near applied load and tendon far from the applied load for specimen S2. Figs. 23 shows Load plotted versus average strain of tendons for all specimens in GI. From the curves, with increasing the applied load eccentricity to increase torsion the average tendon strain increased this is due to increasing warping effect. From the curves, Also, increasing of applied load eccentricity has very slight effect on the ultimate tendon strain.

GII: Figs. 22. b shows Load plotted versus strain for tendon near applied load and tendon far from the applied load for specimen S4. Figs. 24 shows Load plotted versus average strain of tendons for all specimens in GII. It is worth mentioning that, with increasing the tendons initial strain, the linear part of the curve increased. This is due to, increasing the initial compression stress which need a large amount of applied load to open the joint. Form the nonlinear part, all specimens have the same trend as the eccentricity is constant. From the curves, Also, increasing of applied load eccentricity has no effect on the tendon strain due to loading only.

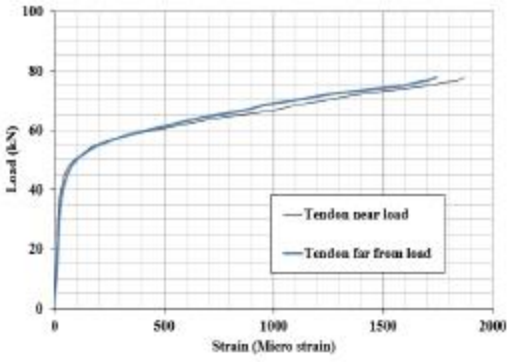

a. specimen S2s-0.5Pys-0.2P

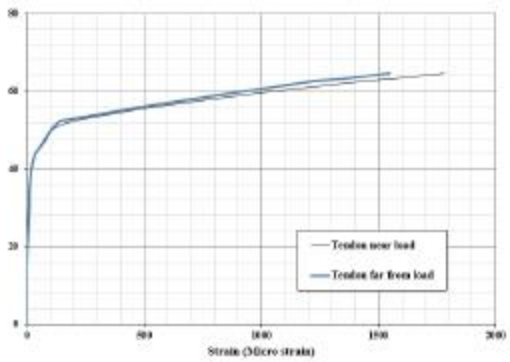

b. specimen S3s-0.5Pys-0.4P

Fig. 22 Load vs. strain of tendons near applied and far from the applied load

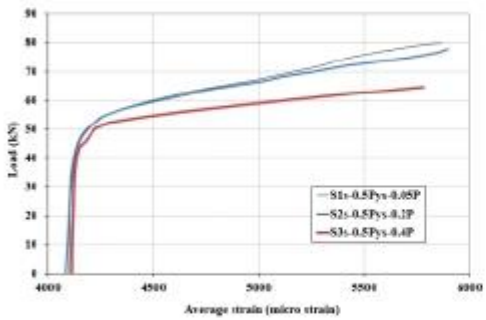

Fig. 23 Load vs. average strain for specimens in GI

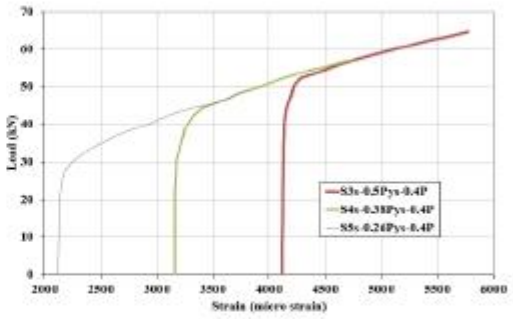

Fig. 24 Load vs. average strain for specimens in GII

concrete strains and opening between segments

This section will take care of the variation of concrete compression strain in compression zone and opening between segments in tension zone with variation of load for all specimens. For concrete strain-load and opening of joint- load relationships, the relationships were initially linear and with increasing the applied load, the response became nonlinear, until failure.

GI: Fig. 25 shows Load plotted versus concrete strain at center of compression face at joint 1 for specimens in GI. Figs. 27 shows Load plotted versus opening of joints between segments at the tension face for joints 1. From the curves, increasing the applied load eccentricity decreases the ultimate concrete strain due to decreasing the ultimate load resistance. From curves, Also, the data prove that the main responsible for the nonlinear behavior of the specimen's tension stresses occurs at the tendons level not mainly the first opening at joints. From chart 25 and at the nonlinear part, at the same load level, with increasing the applied torsion the concrete strain increased and the joint opened faster. Fig. 29 shows comparison curve for the joint opening

(joint 1, 2 and 3) of spacemen S3 behind the start of nonlinear stage, the joints 2,3 closed this is because of the elastic stain at joint 2 and 3 empty out it's strain to the plastic strain regions at joint 1. All specimens behave with the same behavior.

GII: Fig. 26 shows Load plotted versus concrete strain at center of compression face for joint 1 for specimens in GII. Figs. 28 shows Load plotted versus opening of joints between segments at the tension face for joints 1. From the available data of the test, with increasing the initial pre-stressing strain the linear part increases and concrete strain decreases and ultimate concrete strain increased.

SUMMARY OF RESULTS

Form the experimental work, the beam load deflection passed through two main stages; linear stage and nonlinear stage. Linear stage starts with transfer stage then, balanced stage, full prestressing stage, and ends with (partial prestressing stage) allowable stage. The nonlinear stage stats at the end of linear stage and ends with ultimate stage, Fig. 30. Table 3 shows the recorded stages for every specimen.

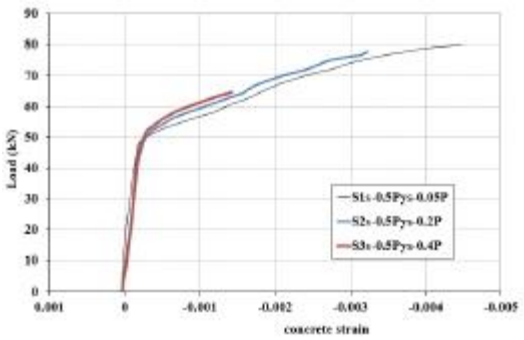

Fig. 25 Load vs. compression concrete strain at the critical joint (compression zone) GI

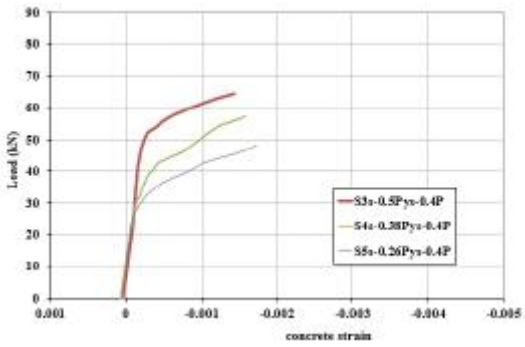

Fig. 26 Load vs. compression concrete strain at the critical joint (compression zone) GII

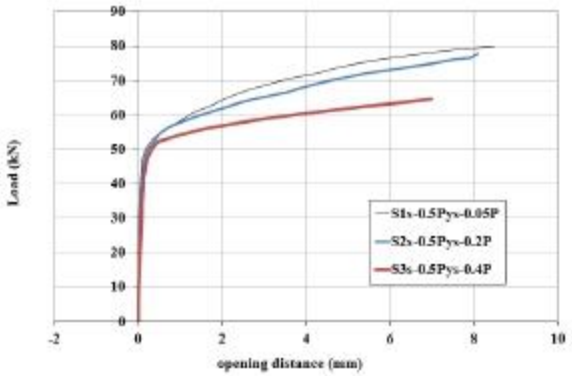

Fig. 27 Load vs. joint opening for the critical joint (Tension zone) GI

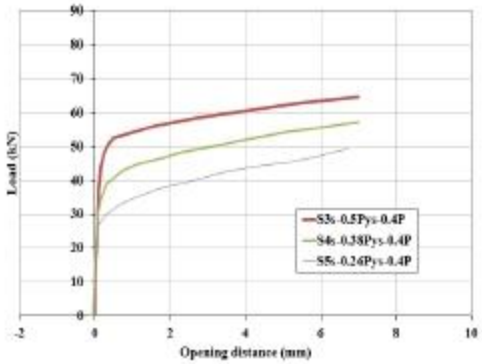

Fig. 28 Load vs. joint opening for joint 3 (Tension zone) GI

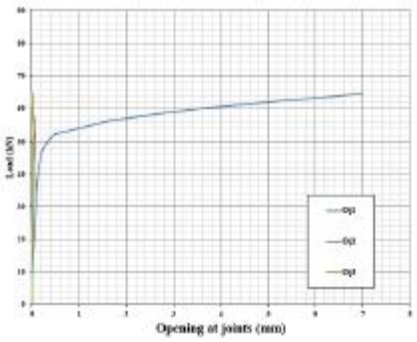

Fig. 29 Load vs. joint opening for the critical joint (Tension zone) GI

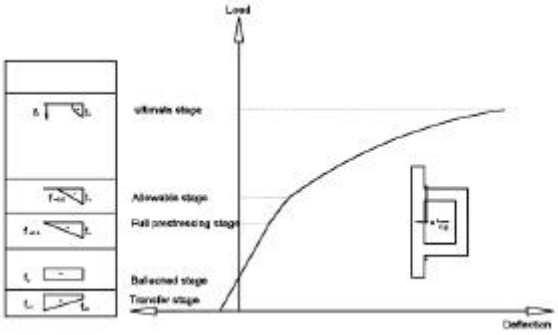

Fig. 30 different loading stages for experimental study

CONCOLOSIONS

The paper summarized the behavior of five segmental box girders with external prestressing. The behavior was evaluated in terms of; load opening joint at max moment, deformations, twist angle, opening between segments, tendon strain, ultimate load capacity, modes of failure, cracks propagation history and some critical values are discussed. From the previous data,

Table 3 The experimentally recorded results and observations

G	specimen	Balanced load (kN)	Full prestressing load (kN)	Allowable load (kN)	Ultimate load capacity (kN)	Failure mode
I	S1s-0.5Pys-0.05P	14.7	42	49.5	79.9	Comp. failure
	S2s-0.5Pys-0.2P	14.7	42.5	49.0	77.86	Comp. failure
	S3s-0.5Pys-0.4P	14.7	42	49.5	64.6	Twisting at joint then Comp. failure
II	S4s-0.38Pys-0.4P	14.7	42	49.5	64.6	Twisting at joint
	S5s-0.26Pys-0.4P	11. 5	32	37.5	57	Twisting at joint
	S1s-0.5Pys-0.05P	7.5	21.5	25.5	49.3	Twisting at joint

1. With increasing the applied force eccentricity to increase the torsion effect, the linear stage ranges not affected. Also, increase the torsion effect at the nonlinear stage has slight effect to decrease the flexural stiffness and decrease significantly the torsional stiffness.
2. With increasing the applied force eccentricity to increase the torsion effect, the ultimate load and ultimate deflection decreased, on contrary, the maximum twist increased.
3. The existing of torsion and its value has significant effect on the beams cracking behavior, deformed shape, mode of failure, and has slight effect on increasing the prestressing steel stress at applied load side more than the side far from the applied load.
4. With increasing the effective pre-stressing force, the linear stage range and ultimate load increased, the ultimate deflection and ultimate twist decreased. Consequently, the prestressing force level has no effect on beam flexural stiffness and torsional stiffness at nonlinear stage.
5. Increasing effective prestressing force level has a significant effect to delay cracking due to shear stresses, and improve the beam deformation against flexure and torsion. Also, it has slight effect to reduce the difference on stresses of tendons at applied load side and tendons far from the applied load side.
6. Opening of joint is not the responsible for the nonlinear behavior. The appearance of tension stress at the joint at the tendon level increase the tendon stress faster and the beam undergo nonlinear behavior.

REFERENCES

[1] G. Rombach, "Precast segmental box girder bridges with external prestressing - design and construction - 2 Structural elements of segmental bridges," Tech. Univ. Hamburg-harbg., vol. 1, no. 1, pp. 1–15, 2002.

[2] ACI Committee 318, Building Code Requirements for Structural Concrete (ACI 318-08), vol. 2007. 2008.

[3] E. G. Nawy, P. L. Solutions, P. C. Edward, N. Solution, M. Edward, E. G. Nawy, C. Solutions, M. Solutions, M. Edward, N. Prestressed, S. Manual, P. Concrete, R. Printing, E. G. Nawy, S. Manual, P. Concrete, F. Edition, C. Version, E. G. Nawy, and E. Engineering, "Edward G Nawy Prestressed Concrete Solution Manual," 2009.

[4] T. Officials, N. C. Street, and N. W. Suite, © 2010 by the American Association of State American Association of State Highway and Transportation Officials Washington , DC 20001 © 2010 by the American Association of State Highway and Transportation Officials . All rights reserved . Duplication is a . 2010.

[5] C. U. S. Units, AAS HTO L RFD B r idg e d e s i g n s p e c i f i c at i o n s. 2012.

[6] S. Specifications, "of Transportation Standard Specifications," no. July, 2016.

[7] H. Farland, "ON THE MECHANICS OF CONTACT AND CRACKING OF SEGMENTAL BEAMS," Raken. Mek. Vol. 23, vol. 23, no. 4, pp. 62–89, 1990.

[8] A. N. A. Hindi, M. E. Kreger, J. E. Breen, and T. P. Division, "External Post-Tensioned Bridgeu," ·U.S. Dep. Transp. Fed., vol. 7, no. 2, 1991.

[9] C. L. Roberts, E. Breen, M. E. Kreger, and T. T. Office, "MEASUREMENT BASED REVISIONS FOR SEGMENTAL," Dep. Transp., vol. 7, no. 2, 1993.

[10] A. C. Aparicio, "ULTIMATE ANALYSIS OF MONOLITHIC AND SEGMENTAL EXTERNALLY," J. Bridg. Eng., pp. 10–17, 1996.

[11] M. K. Thompson, R. T. Davis, J. E. Breen, and M. E. Kreger, "MEASURED BEHAVIOR OF A CURVED PRECAST SEGMENTAL CONCRETE BRIDGE ERECTED BY BALANCED CANTILEVERING," TEXAS Dep. Transp., vol. 7, 1998.

[12] A. C. Aparicio, G. Ramos, and J. R. Casas, "Testing of externally prestressed concrete beams," Eng. Struct., vol. 24, no. 1, pp. 73–84, 2002.

[13] J. Turmo, G. Ramos, and A. C. Aparicio, "FEM study on the structural behaviour of segmental concrete bridges with unbonded prestressing and dry joints : Simply supported bridges," Eng. Struct., vol. 27, pp. 1652–1661, 2005.

[14] T. Aravinthan, E. Witchukreangkrai, and H. Mutsuyoshi, "Flexural Behavior of Two-Span Continuous Prestressed," Aci Struct. J., no. 102, 2006.

[15] J. Turmo, G. Ramos, and A. C. Aparicio, "FEM modelling of unbonded post-tensioned segmental beams with dry joints," Eng. Struct., vol. 28, pp. 1852–1863, 2006.

[16] "Finite element model updating of a segmental box girder based on measured responses under load testing," 6th Int. Work. Struct. Heal. Monit. Stanford Univ, Stanford, CA, pp. 459–466, 2007.

[17] A. Rombach and R. Abendeh, "Bow-shaped segments in precast segmental bridges," Eng. Struct., vol. 30, pp. 1711–1719, 2008.

[18] E. Engineering, "SEISMIC DESIGN AND ANALYSIS OF PRECAST SEGMENTAL CONCRETE BRIDGE SUPERSTRUCTURE," Univ. degli Stud. di Pavia, vol. Master Deg, 2009.

[19] M. F. Granata, D. Ph, M. Asce, A. Recupero, and D. Ph, "Serviceability and Ultimate Safety Checks of Segmental Concrete Bridges through N - M and M - V Interaction Domains," ASCE, J. Bridg. Eng, vol. B4014003-1, pp. 1–11, 2009.

[20] R. Malm and H. Sundquist, "Time-dependent analyses of segmentally constructed balanced cantilever bridges," Eng. Struct., vol. 32, no. 4, pp. 1038–1045, 2010.

[21] R. G. Pillai, M. D. Hueste, P. Gardoni, D. Trejo, and K. F. Reinschmidt, "Time-variant service reliability of post-tensioned , segmental , concrete bridges exposed to corrosive environments," Eng. Struct., vol. 32, no. 9, pp. 2596–2605, 2010.

[22] F. T. K. Au and C. C. Y. Leung, "Full-Range Analysis of Multi-Span Prestressed Concrete Segmental Bridges," Procedia Eng., vol. 14, pp. 1425–1432, 2011.

[23] A. Yuan, H. Dai, D. Sun, and J. Cai, "Behaviors of segmental concrete box beams with internal tendons and external tendons under bending," Eng. Struct., vol. 48, pp. 623–634, 2013.

[24] A. Yuan, Y. He, H. Dai, and L. Cheng, "Experimental Study of Precast Segmental Bridge Box Girders with External Unbonded and Internal Bonded Posttensioning under Monotonic Vertical Loading," J. Bridg. Eng, ASCE, vol. 20, no. 4, pp. 1–12, 2015.

[25] H. Jiang, Q. Cao, A. Liu, T. Wang, and Y. Qiu, "Flexural behavior of precast concrete segmental beams with hybrid tendons and dry joints," Constr. Build. Mater., vol. 110, pp. 1–7, 2016.
[26] K. Deeprasertwong and Y. W. Leung, "full-scale destructive test of a precast segmental box girder bridge with dry joints and external tendons," Struct. Build. Boord Struct. Panel Pap. 10452, vol. 104, no. 10452, pp. 297–315, 1994.
[27] G. C. Lacey and E. Breen, "LONG SPAN PRESTRESSED CONCRETE BRIDGES OF SEGMENTAL CONSTRUCTION," Texas Highw. Dep., vol. Research R, no. May 1969.
[28] B. G. Rabbat, "Testing of Segmental Concrete Girders With External Tendons," PCI JOURNAU, pp. 86–107.
[29] C. Sivaleepunth, J. Niwa, D. H. Nguyen, T. Hasegawa, and Y. Hamada, "SHEAR CARRYING CAPACITY OF SEGMENTAL PRESTRESSED CONCRETE BEAMS," Doboku Gakkai Ronbunshuu, vol. 65, no. 1, pp. 63–75, 2009.
[30] T. Paper, "INFLUENCE OF PRSTRESS LEVEL ON SHEAR BEHAVIOR OF," Tech. Pap., vol. 31, no. 2, 2009.
[31] J. N. and T. H. Dinh Hung NGUYEN1, Ken WATANABE2, "MODIFIED MODEL FOR SHEAR CARRYING CAPACITY OF SEGMENTAL CONCRETE BEAMS WITH EXTERNAL TENDONS," Doboku Gakkai Ronbunshuu, vol. 66, no. 1, pp. 53–67, 2010.
[32] W. Yabuki, H. Otsuka, and T. Wakasa, "Experimental study of the shear strength of precast segmental beams with external prestressing," Struct. Concr., vol. 6, no. 2, pp. 63–80, 2005.
[33] M. A. Al-Gorafi, A. A. A. Ali, I. Othman, M. S. Jaafar, and M. P. Anwar, "Externally Prestressed Monolithic and Segmental Concrete Beams under Torsion: a Comparative Finite Element Study," IOP Conf. Ser. Mater. Sci. Eng., vol. 17, p. 12041, 2011.
[34] M. A. Algorafi, A. A. A. Ali, I. Othman, M. S. Jaafar, and R. A. Almansob, "Evaluation of Structural Behavior of Externally Prestressed Segmented Bridge with Shear Key under Torsion," vol. 1, no. 1, pp. 28–35, 2011.
[35] M. A. Algorafi, A. A. A. Ali, I. Othman, M. S. Jaafar, and M. P. Anwar, "Experimental study of externally prestressed segmental beam under torsion," Eng. Struct., vol. 32, no. 11, pp. 3528–3538, 2010.
[36] M.P. Anwar and . Rashid Algorafi, M.A., Ali, M.S. Jaafar,. Othman, "Effect of Torsion on Externally Prestressed Segmental Concrete Bridge with Shear Key," Am. J. Eng. Appl. Sci., vol. 2, no. 1, pp. 54–60, 2009.